Effect of Surface Distortions on the Heat Transfer to a Wing at Hypersonic Speeds

MITCHEL H. BERTRAM* AND M. MARGARETTE WIGGS†

NASA Langley Research Center, Hampton, Va.

Sources of disturbances to the surface flow on hypersonic vehicles may result from local distortions due to aerodynamic heating effects on the structure and skin. The effects of surface distortions, consisting of slots, small steps, and local curvatures, on the heat-transfer and surface pressures on a wing with a thick boundary layer at hypersonic speeds are examined. The results of experiments on an unswept slab wing at nominal freestream Mach numbers of 7 and 10 show the effect of these surface distortions on heating and surface pressure at angles of attack up to 20°. This wing, with both blunt and sharp leading edges, gives results over a wide range of local Reynolds and Mach numbers. Important alterations to the heat-transfer distribution were obtained from these surface distortions.

Nomenclature

c_m = specific heat of skin material
h = film coefficient of heat transfer, $h = q/(T_e - T_w)$
H = distortion maximum height or depth
k_m = thermal conductivity of skin
M = Mach number
N_{St} = Stanton number
p = static pressure
q = surface heat-transfer rate
R = Reynolds number
R_s = Reynolds number based on length from geometric stagnation point
R_t = Reynolds number based on diameter of cylindrical leading edge
s = surface distance from geometric stagnation point
s_0 = surface distance from midline of cylindrical leading-edge slab
T = temperature
t = diameter of cylindrical leading edge
t_m = thickness of model skin material
α = angle of attack
δ^* = displacement thickness of boundary layer
ρ_m = density of model skin material
τ = time

Subscripts

e = adiabatic wall
fp = flat plate
w = skin
max = maximum
0 = stagnation
l = local
∞ = undisturbed freestream
L = laminar

Introduction

IN calculations of the heating load on hypersonic vehicles, analyses generally are resorted to which assume that the vehicle has a smooth surface. In the practical case, however, when the vehicle surface is subjected to large heating rates and high temperatures, the surface may distort locally and thus leave open to considerable question, the validity of calculations that do not take these distortions into account. There are also cases where this surface distortion is the result of a particular choice of structural design and a combination of design approach and high temperatures.

In order to investigate the problem of local surface disturbances on the surface pressure and heat transfer, a program was undertaken to determine the effect of simple distortions to the surface of a flat plate. These surface distortions consisted of slots, small steps, and local curvatures in the surface. The experiments were run in the Langley 11-in. hypersonic tunnel at freestream Mach numbers of 6.8 and 9.6 at angles of attack up to 20°. This plate was tested with interchangeable sharp and cylindrically blunted leading edges.

Test Apparatus and Models

The experiments were conducted in the Langley 11-in. hypersonic tunnel. The Mach number in this blowdown facility can be varied by changing nozzles. In the present tests, nozzles giving nominal Mach numbers of 6.8 and 9.6 with air as the test medium were used. The Mach number 6.8 nozzle is a contoured two-dimensional nozzle machined from Invar to minimize deflection of the nozzle throat due to thermal gradients.[1] The Mach number 9.6 nozzle is a contoured three-dimensional nozzle with a square throat and test section.[2]

The model used in this investigation was a slab wing of which a portion was removable so that pieces containing the distortion shapes to be tested could be inserted as shown in Fig. 1. This slab had two interchangeable leading edges, one sharp (thickness about 0.001 in.) and the other a hemicylinder with a diameter of 0.75 in. The material of which the slab and the inserts were constructed was 321 stainless steel except for the leading-edge pieces that were of 17-7 stainless steel. Removable sharp-edged end plates with the front end shaped to the shock from the cylindrical leading edge were provided also.

The surface distortion inserts that contained the pressure and thermocouple leads are detailed in Fig. 2. There were a total of eight inserts of which one was a flat insert for comparative purposes. The results from these inserts could, in general, be classed as two dimensional, except for those from the longitudinal slot insert (Fig. 2a). As shown in Fig. 2, the shapes tested ranged from sharp-edged steps and lateral and longitudinal slots (Fig. 2a) to a sine curve of one wavelength arranged in various ways (Fig. 2b).

Heat-transfer data were obtained through the use of chromel-alumel thermocouples from the transient temperatures near the start of a test run by a quick starting technique that approximates the sudden immersion of the model in a fully developed test-section flow. The data were obtained at average stagnation temperatures of 1140° R and 1565° R at the Mach numbers of 6.8 and 9.6, respectively, and a wall temperature of about 560° R. The thin-skin equation for the

Presented at the IAS Annual Summer Meeting, Los Angeles, Calif., June 19–22, 1962.

* Head, Hypersonic Branch. Associate Fellow Member AIAA.
† Mathematician, Hypersonic Aerodynamic Section.

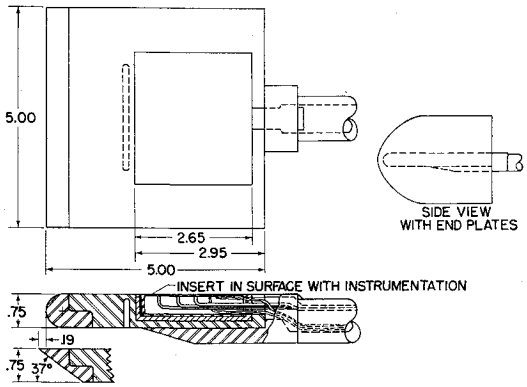

Fig. 1 Sketch of slab model used in surface distortion study

local heating rate $q = c_m \rho_m t_m dT_w/d\tau$ was used in which c_m was taken as 0.12 Btu/lb-°F, ρ_m as 0.288 lb/in.^{3} and t_m was a measured local skin thickness generally not deviating from 0.020 in. by more than ± 0.002. The finite time required for the proper flow conditions to be established in the nozzle was such that the temperature rise of the inserts was sufficient to require conduction corrections on all the inserts but the flat-plate one. A two-dimensional conduction correction was used with the required second derivative of surface temperature with surface distance evaluated by a three-point finite difference method and the thermal conductivity of the skin material given by

$$k_w = [0.00118T_w(°R) + 1.33] \times 10^{-4}, \text{ Btu/(sec.-in.-°F)}$$

For reducing the thermocouple results to Stanton number, the adiabatic wall temperature used is shown in Fig. 3 as a

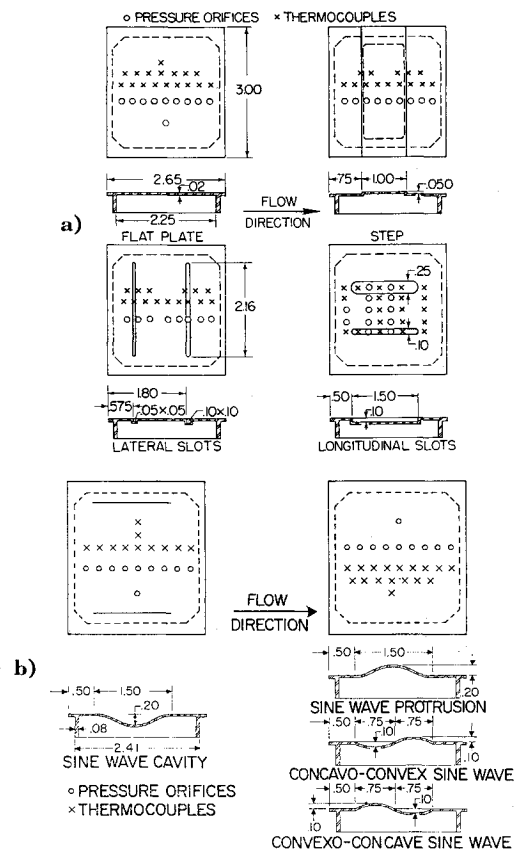

Fig. 2 Sketch of insert shapes for surface distortion study; a) flat plate, step, and slot inserts, b) sine wave contour inserts

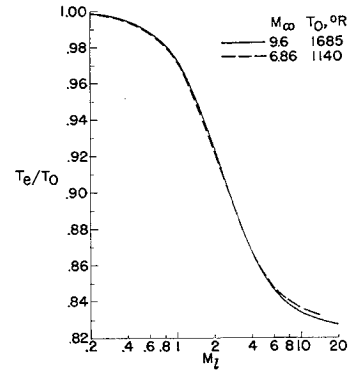

Fig. 3 Calculated laminar recovery temperature ratio

function of the local Mach number. This adiabatic wall temperature was calculated from the Prandtl number corresponding to Monaghan's laminar T-prime temperature for an insulated plate as outlined in Ref. 3. The calculations indicate a negligible difference between the different freestream Mach numbers for a given local Mach number. The local Mach number was obtained from curves like those shown in Fig. 4 using the measured pressures. The laminar displacement thickness shown in nondimensional form in Fig. 5 also was calculated by the Monaghan T-prime method. As used later in this paper, though local pressure was considered, pressure gradients were not taken into account in estimating boundary layer displacement thickness based on indications from similarity theory.[2, 3] For the cylindrical leading edge, the boundary layer was assumed always to be immersed in an entropy layer due to a normal shock at the model leading edge.

Figure 6 gives estimates of the Reynolds numbers in the entropy layer (but outside the boundary layer) as a function of surface pressure.

Results and Discussion

Effect of End Plates—Surface Flow

One of the problems in obtaining valid data from the distortion inserts was that of eliminating, as much as possible, extraneous phenomena from affecting the results. One concern was that of insuring two-dimensional flow over the plate. Previous work done in the Langley 11-in. hypersonic tunnel had indicated a strong effect of edge proximity on the surface shear direction. The plate tested was of solid metal with a cylindrical leading edge of the same thickness as in the present investigation, 0.75 in., but 6-in. square instead of 5-in. square. As shown on the right in Fig. 7a, for zero angle of attack at a Mach number of 9.6, oil streak lines indicate outward flow as the high pressures induced by the blunt leading edge are relieved by the edges. The addition of end plates shaped to the leading-edge shock gives essentially straight streak lines though there is an indication of a disturbance at the edges introduced by the end plates. (The same end plates shown in

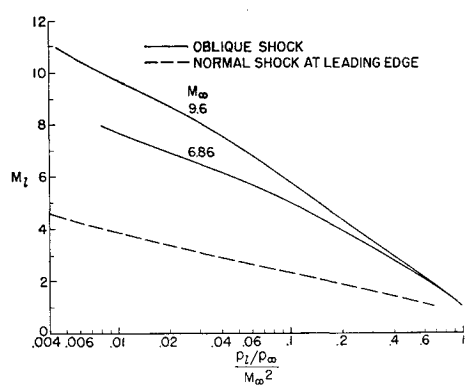

Fig. 4 Calculated local Mach number

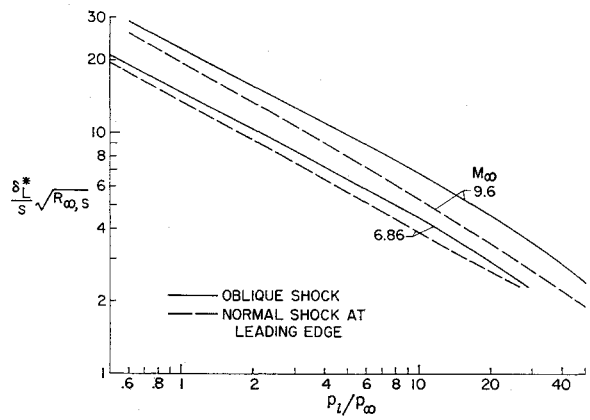

Fig. 5 Calculated laminar boundary layer displacement thickness, $T_w = 560°R$

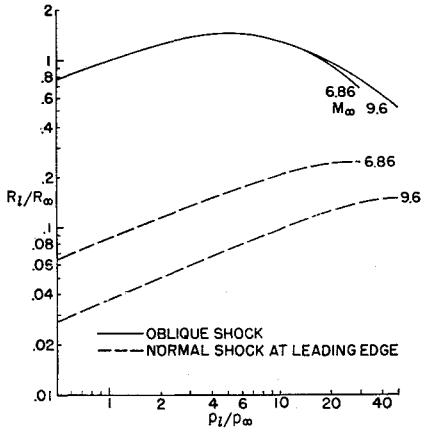

Fig. 6 Calculated local Reynolds number

Fig. 1.) The result was much the same at 10° angle of attack as shown by the surface flow patterns in Fig. 7b.

Effect of End Plates—Pressures and Heat Transfer

The effect of the end plates on the surface pressures is shown in Fig. 8a for the flat-plate insert and three of the distortions as a function of surface distance (from the midline of the wing) for the cylindrically blunted wing. There is definitely a tendency for the pressures to be slightly lower for the wing without end plates though the effect is small enough so that the same conclusions concerning the effect of the surface distortions would be arrived at whether considering the data with or without end plates. This remark also would hold for the equivalent heat-transfer data presented in Fig. 8b. Here, there generally is shown a slight increase in heat transfer for the data obtained without end plates as compared to that from the model with end plates.

The same result noted in Ref. 4 readily may be discerned by comparing Figs. 8a and 8b, that is, the changes in heat transfer caused by a distortion to the plate surface are in these cases at least much larger percentagewise than the changes in pressure.

Flat-Plate Pressures—Cylindrical Leading Edge

The surface pressure results from the flat-plate insert are compared with previously obtained results, on a slab having a leading edge of the same thickness but 6-in. long, in Fig. 9. The solid points are the previous data obtained in the Langley 11-in. hypersonic tunnel both unpublished and published[3, 5] and the unfilled data points are from the flat-plate insert of the present investigation. Generally, good agreement is obtained between the different sets of data, where they over-

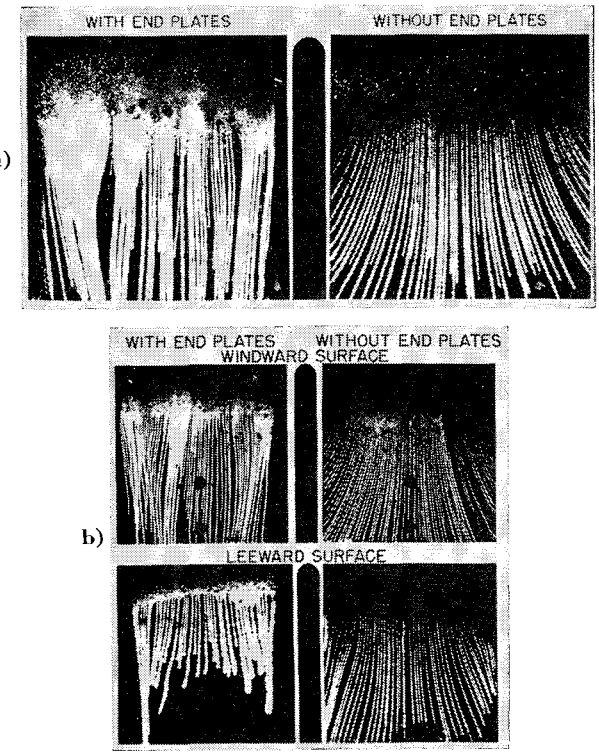

Fig. 7 Effect of end plates on surface flow over smooth slab, $M_\infty = 9.6$, $R_{\infty,t} \approx = 8 \times 10^4$; a) α 0°, b) $\alpha = 10°$

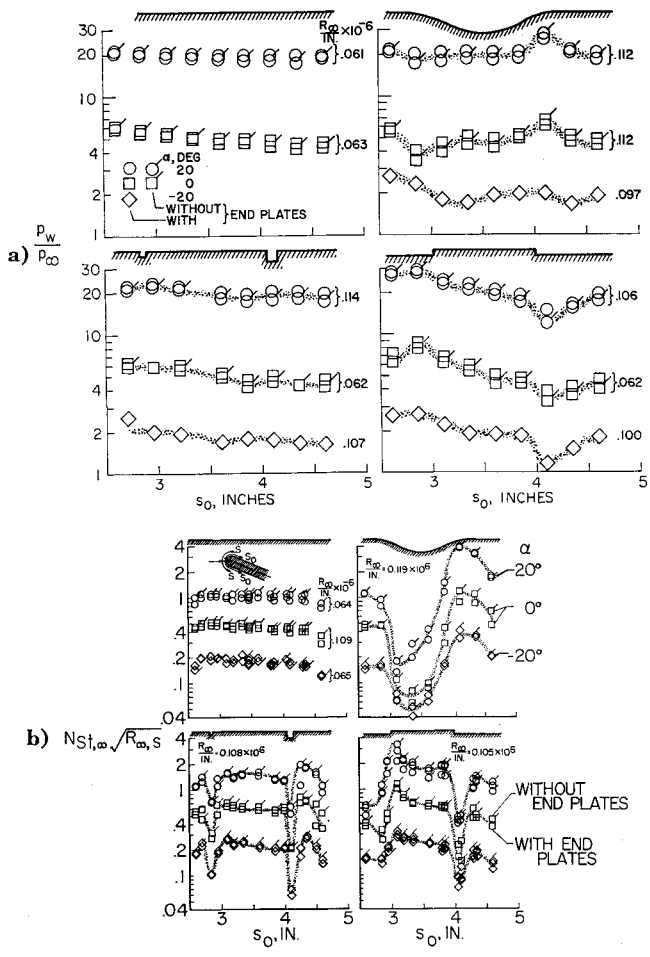

Fig. 8 Effect of end plates on pressure and heat-transfer distribution. Cylindrical leading edge, $M_\infty = 9.6$; a) pressures, b) heat-transfer parameter

lap, at Mach numbers of 6.8 and 9.6. In addition, there is good prediction of the data by the results from characteristics theory. The characteristics theory uses the sonic-wedge leading edge to start the solution, and the numerical results are corrected to the drag coefficient of a cylindrical leading edge according to the indication of blast-wave theory.[6, 7]

Effect of Surface Distortions on the Heating Distribution

Examples of the sort of Stanton number distributions obtained for four of the surface distortions studied are shown in Fig. 10. Results are shown at zero angle of attack for both the sharp and blunt leading-edge plate at the Mach numbers of 6.8 and 9.6. The flat-plate laminar heat-transfer correlation parameter, Stanton number times square root of Reynolds number based on freestream conditions, is plotted vs surface distance freestream Reynolds number. There are results at several unit Reynolds numbers and the flat-plate results given by the open symbols are included for comparison.

Results from the step insert that consists of a forward facing step followed by a rearward facing step with a flat 20 step heights long joining the two are shown in Fig. 10a. The measurements show a large increase in heating on the step. The peak of this increase occurs at the top of the step and rapidly declines from this point. Immediately behind the rearward facing step, the heating rate drops to roughly half that of the flat plate at the same location but quickly rises again to about the flat-plate value.

For the sine wave cavity, the measurements give the heating distributions shown in Fig. 10b. Oil-flow patterns indicate that separation occurs a short distance after the start of the sine wave proper and the flow does not reattach until the end of the sine wave cavity. In the cavity, the heat transfer drops to a minimum of roughly $\frac{1}{6}$ the flat-plate value (on the

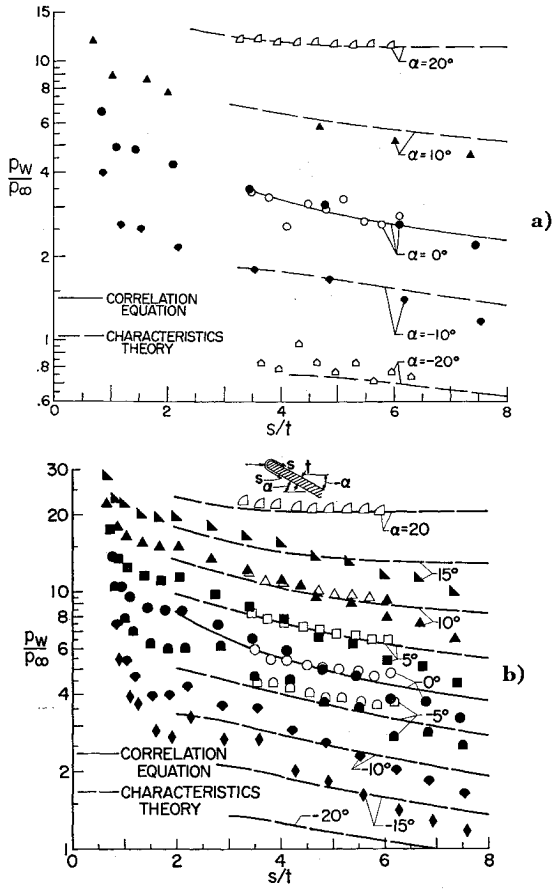

Fig. 9 Pressure distribution on smooth slab with cylindrical leading edge; a) $M_\infty = 6.8$, $R_{\infty,t} = (0.8\text{–}3.1) \times 10^5$; b) $M = 9.6$, $R_{\infty,t} = 8 \times 10^4$

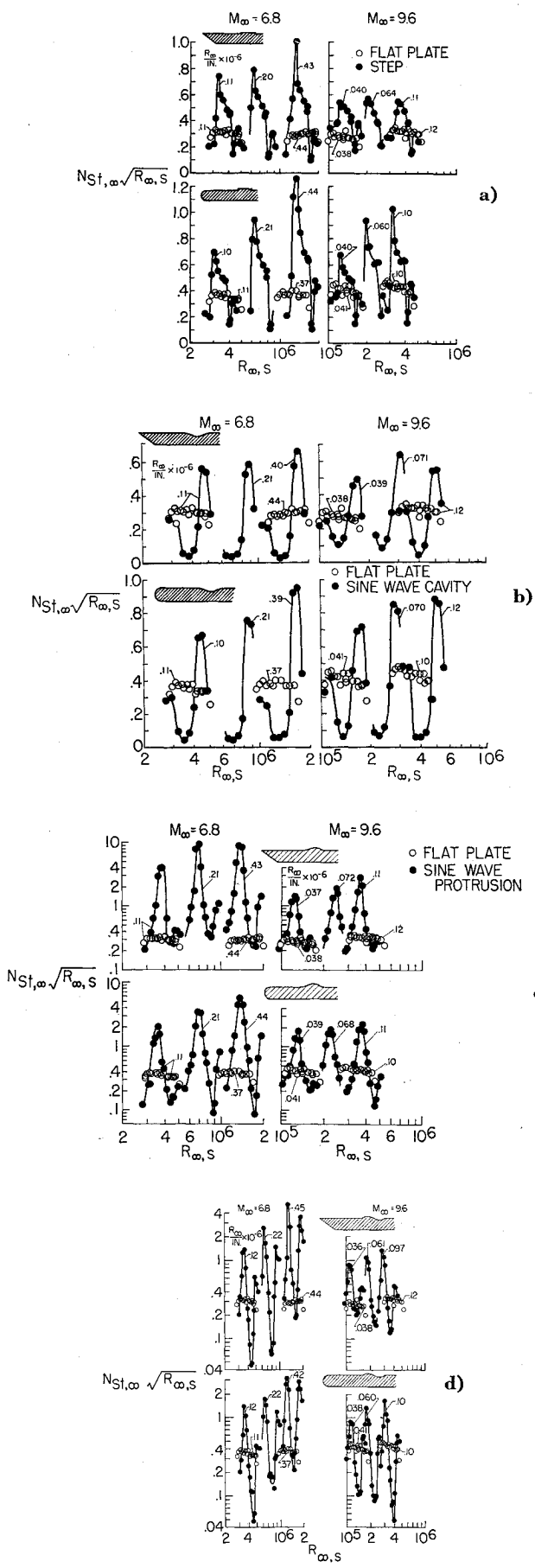

Fig. 10 Heating distribution on surface distortion inserts at various unit Reynolds numbers, $\alpha = 0°$; a) step insert, b) sine wave cavity insert, c) sine wave protrusion insert, and d) convexo-concave sine wave insert

average) just ahead of the center of the cavity. After the minimum in heating, the Stanton number parameter increases rapidly to a value much greater than the flat-plate value and the peak heating occurs at the point of reattachment. For much of the range of conditions investigated, the total heating load for the cavity and vicinity was roughly the same as for the smooth flat plate though the heating distribution was radically changed.

The sine wave protrusion has the same dimensions as the sine wave cavity though reversed in sign. Oil-flow studies indicate separations that extend well ahead of the insert, in fact, as much as half way to the leading edge ahead of the actual distortion to the surface. In general, the heat-transfer distributions shown in Fig. 10c indicate a lower heat transfer than on a flat plate in this separated region but the heat transfer rapidly increases to values many times the flat-plate value in the region of reattachment. In this case, there is a second separation after the flow expands around the crest of the sine wave. In this second separated region, the heat transfer drops well below the flat-plate value but quickly rises again further downstream. At the higher Reynolds number at a freestream Mach number of 6.8 the heat transfer further increases to large values above the flat-plate value. This second increase may be due to transition of the boundary layer. It is interesting to note that the oil-flow studies indicate what appear to be paried vortices that cover the rear of the insert and extend the entire span of the insert at the highest unit Reynolds number at Mach number 6.8. Similar three-dimensional oil-flow patterns occur on the front part of the convex sine wave when transitional flow is found there. This phenomenon is similar to that reported by Thomann[8] on rearward facing steps.

Heating distributions for the convexo-concave sine wave distortion are shown in Fig. 10d. In this case, oil flow indicates separation ahead of the forward protruding portion of the sine wave, reattachment ahead of the maximum height, and a second separation that bridges the cavity about level with the external flat surface. In line with the oil-flow indications, there is a region of low heat transfer ahead of the protruding surface. The heat transfer increases as one moves back onto the protrusion and peaks at about the place where reattachment occurs. From this peak, the heating drops rapidly in the expansion around the protrusion until values well below those on the flat plate are obtained under the separated flow in the cavity. However, the flat-plate heating values generally are attained or exceeded before the end of the cavity. The high heating values at the highest unit Reynolds numbers at Mach number 6.8 for these rear stations may be due to transition induced by the distortion.

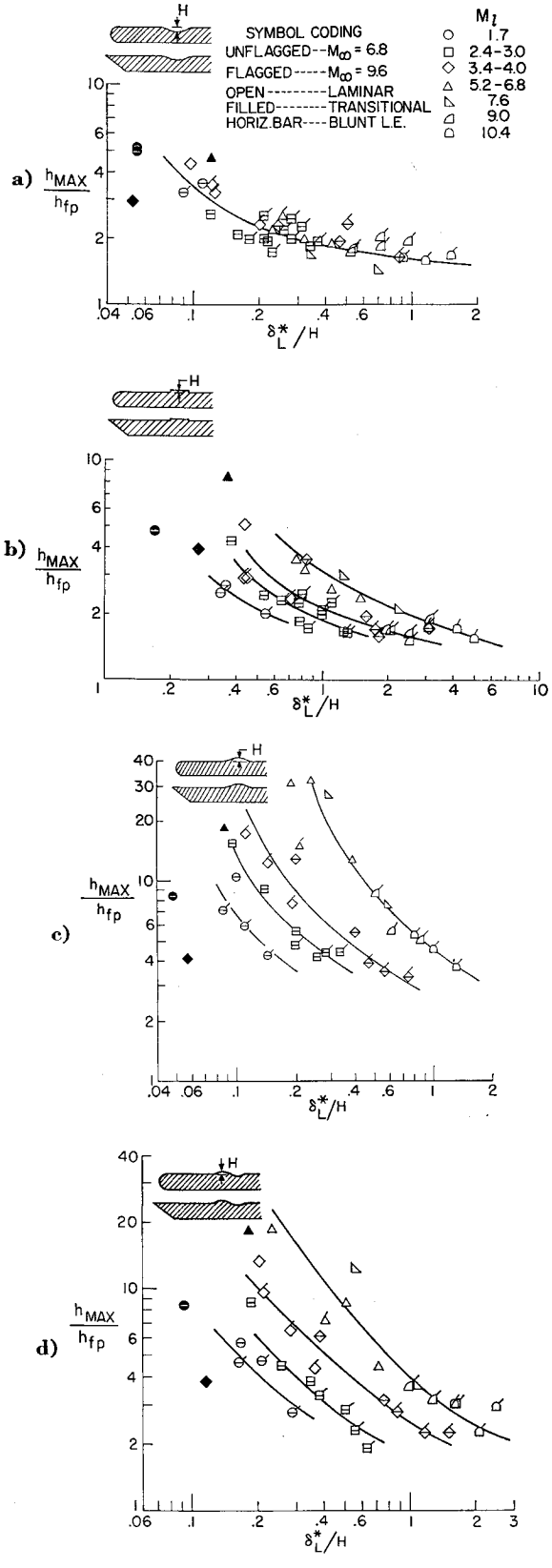

Fig. 11 Peak heating on surface distortion inserts as a function of laminar boundary layer displacement thickness; a) sine wave cavity insert, b) step insert, c) sine wave protrusion insert, and d) convexo-concave sine wave insert

Effect of Estimated Boundary Layer Displacement Thickness on the measured peak heating

Boundary layer thickness suggests itself as one possible criterion for correlating or comparing results. Actually, because of the difficulty in defining boundary layer thickness itself, the displacement thickness would appear to be a better

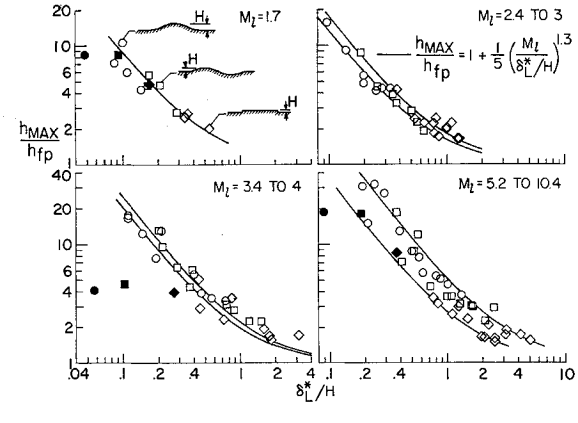

Fig. 12 Peak heating on protruding surface distortion inserts as a function of laminar boundary layer displacement thickness. Solid points indicate transitional data based on evidence from flat-plate insert

choice and thus was used. The displacement thicknesses used were not measured but were calculated as explained in an earlier section and these calculated curves were shown in Fig. 5. The estimated laminar displacement thickness on the flat plate was used as a criterion at the equivalent distance where the peak in aerodynamic heating occurred on the surface distortion. This thickness was normalized by the maximum height or depth dimension of a given distortion. The peak film coefficient of a given distribution of heating was nondimensionalized by dividing by the measured film coefficient for the flat plate at the same distance from the leading edge under equivalent conditions of flow and model orientation. For presentation in this manner, the data were divided into groups of similar local Mach number according to the curves in Fig. 4, using the equivalent flat-plate surface pressure. Transition is known to have occurred on the flat-plate insert for data obtained at several of the highest Reynolds numbers at freestream Mach number 6.8 and angles of attack of 10° and 20°. In these cases the ratio of the measured film coefficients was used still but this ratio was plotted against the estimated laminar displacement thickness.

The result of arranging the data in this manner is shown in Fig. 11 for four of the surface distortions. The peak heating ratio for the sine wave cavity is presented in Fig. 11a. For this surface distortion shape, the peak heating is a function of the boundary layer thickness but does not appear to be a function of the local Mach number. For a boundary layer thickness about $\frac{1}{10}$ of the cavity depth, the peak heating is 3 or 4 times that at the same place on a flat plate. However, the peak heating decreases with increasing boundary layer thickness and is approaching a 50% increase for a boundary layer thickness about double the cavity depth. The transitional data shown in black do not indicate any radical departure from the laminar data. It should be emphasized that the label of transitional data is based on results from the flat plate. If the flat-plate results are laminar but the distortion itself causes transition to occur, this would not be known from Fig. 11.

For the step distortion results in Fig. 11b, the peak heating is found to be a function of both local Mach number (on comparable flat plate) and boundary layer thickness. Again a thinner boundary layer results in increased heating (at a given local Mach number), but also at a fixed boundary layer thickness an increase in the local Mach number is associated with an increase in the peak heating.

The sine wave protrusion results in Fig. 11c show the same sort of dependence on local Mach number and boundary layer thickness as the step distortion; however, the actual magnitude of the peak heating over that on the flat plate is many times greater than obtained on the step. Here the peak heating is up to 30 times greater than on the flat plate. With a boundary layer thickness somewhat greater than the height of the protrusion, the peak heating was still about 4 times the flat-plate value. Much of this increase in peak heating for the sine wave protrusion over that obtained on the step must be attributable to the greater height of the protrusion. The sine wave protrusion is 4 times the height of the step.

In order to check further the effect of distortion height, data from the convexo-concave distortion were examined in this same way and the results are shown in Fig. 11d. In this case, the maximum height of the protrusion is twice that of the step protrusion. The peak heating ratios are intermediate between the step and the sine wave protrusion results and occur at about the place of reattachment on the forward protruding surface.

To determine similarities or differences between the peak heating ratios on these three protruding distortions (the sine wave, step, and convexo-concave protrusions), these data were collected together and plotted in the same way as for Fig. 11. In Fig. 12, these data for the various protuberances are presented for given ranges of local Mach number. Interestingly enough, the peak heating ratio as a function of boundary layer thickness ratio is about the same for these three distortions. (Again the solid points indicate those data where, at least, the comparable flat-plate data were known to be in the transitional range.) A simple empirical relation

$$\frac{h_{\max}}{h_{fp}} = 1 + \frac{1}{5}\left(\frac{M_l}{\delta_L^*/H}\right)^{1.3}$$

was found to represent the peak heating data from the three protuberant distortions.

Concluding Remarks

An experimental study was done at hypersonic Mach numbers to determine the effect of simple distortions on the heating and pressure distributions on a plate. These distortions were mainly two dimensional in nature. Probably as much as anything else, this study indicates the need for information over an even larger range of conditions than were possible to obtain here, and over more extensive regions of the surface before and behind the surface distortions than were instrumented in this investigation. From the results of this study, the following observations were made.

For the step distortion consisting of forward facing step followed by a rearward facing step with a flat, 20 step heights long, joining the two there was a large increase in heating on this flat. This increase appears to be a function of the local Mach number and the boundary layer displacement thickness. However, even with estimated displacement thicknesses 2 to 5 times the step height, the maximum heating recorded on top of the step was still 50% greater than on the smooth flat plate at high local Mach numbers.

For a sine wave shape cavity, there was an initial decrease in heating as the flow started to expand into the cavity and then separated. There was, however, a large increase in the heating in the region of reattachment whose maximum appeared to be a function of boundary layer thickness only. The thicker the displacement thickness, the less the increase in heating. For much of the range of conditions investigated, the total heating over the cavity length did not appear to be much different than over the same length of smooth flat plate though the heat was radically redistributed. However, as noted by Bogdonoff and Vas for cavity flows, it is not enough to examine only the cavity itself, but the effect of the cavity on the surface away from the cavity must be determined.

The sine wave shape protrusion had a large effect on the heating rate. The peak heating was up to 30 times greater than over the smooth flat plate for the thinner boundary layers and was still about 4 times the flat-plate value with an estimated displacement thickness somewhat greater than the protrusion height.

There was considerable difference in heating results between that distortion that was essentially a cavity and those distortions that protruded above the surface. Those which protruded seemed to have effects that were a considerable function of the local Mach number, whereas the cavity results appeared to be independent of local Mach numbers where boundary layer displacement thickness was used as a criterion. All the distortions investigated caused at least high local increases in aerodynamic heating which could be dangerous in flight.

The protuberant distortions though having considerably different heating distributions from each other were found to have about the same increase in peak heating where the ratio of boundary layer thickness to protuberance height was the same. The variation in peak heating with boundary layer thickness ratio was found to be represented by a simple empirical equation for the range of conditions of these tests.

As a general remark, it can be said that the surface distortions had a much smaller effect on local pressures than on the local heating.

References

[1] Bertram, M. H., "Exploratory investigation of boundary-layer transition on a hollow cylinder at a Mach number of 6.9," NACA Rept. 1313 (1957); supersedes NACA TN 3546.

[2] Bertram, M. H., "Boundary-layer displacement effects in air at Mach numbers of 6.8 and 9.6.," NASA TR R-22 (1959); supersedes NACA TN 4133.

[3] Bertram, M. H. and Feller, W. V., "A simple method for determining heat transfer, skin friction, and boundary-layer thickness for hypersonic laminar boundary-layer flows in a pressure gradient," NASA Memo. 5-24-59L (1959).

[4] Bogdonoff, S. M. and Vas, I. E., "Some experiments on hypersonic separated flows," ARS J. **32**, 1564–1572 (1962).

[5] Bertram, M. H. and Henderson, A., Jr., "Recent hypersonic studies of wings and bodies," ARS J. **31**, 1129–1139 (1961).

[6] Bertram, M. H. and Baradell, D. L., "A note on the sonic-wedge leading-edge approximation in hypersonic flow," J. Aeronaut. Sci. **24**, 627–628 (1957).

[7] Baradell, D. L. and Bertram, M. H., "The blunt plate in hypersonic flow," NASA TN D-408 (1960).

[8] Thomann, H., "Measurements of heat transfer and recovery factor in regions of separated flow at a Mach number of 1.8," Aeronaut. Res. Inst. Sweden (FFA), Rept. 82 (1959).

JUNE 1963 AIAA JOURNAL VOL. 1, NO. 6

Particulate Damping of Oscillatory Combustion

M. D. HORTON* AND M. R. MCGIE†
U. S. Naval Ordnance Test Station, China Lake, Calif.

An experiment is described in which the attenuation of oscillatory burning by aluminum is studied by means of a self-excited, one-dimensional oscillatory burner. Values of the response function of the combustion zone are presented for several variations of a composite propellant, which differ only in that some contain small amounts of aluminum. The data show that the addition of a small amount of aluminum to the propellant tested has little or no effect upon the response function of the flame (as defined by the Hart-McClure theory). These data show also that, for this experimental system, there is an increased acoustic damping that is caused by the presence of aluminum in the propellant. If this increased damping is ascribed to the formation of condensed Al_2O_3 droplets in the combustion gas, it is shown that the theory of Epstein and Carhart can explain the increased damping. As a function of frequency, the variables tested in the experimental program were three different aluminum additives, four concentrations of alumina, alumina as an additive, and the effect of pressure.

Nomenclature

A_a = viscous attenuation length as defined by Eq. (4); this constant is positive for positive damping
c = velocity of sound in combustion gas
E = acoustic energy density
f = frequency of oscillations during their growth, cps
f_d = average frequency of oscillations during their decay, cps
i = $-1^{1/2}$
n_D = number of particles per unit volume with diameter D
P = mean chamber pressure during firing in the burner
p = instantaneous acoustic pressure
p_0 = amplitude of pressure oscillations at arbitrary zero time
r = linear burning rate of solid propellant
R = radius of particle in combustion gas
t = time
u = fractional mass perturbation caused by fractional pressure perturbation ϵ
y = reduced specific acoustic admittance of combustion zone
Z = $(\omega R^2/2\nu)^{1/2}$
α = constant that describes exponential change in amplitude of oscillations with time
α_a = damping constant ascribed to particulate viscous damping; a negative value indicates positive damping
α_c = growth rate constant due to oscillatory driving of combustion zone
α_d = damping constant that includes all sources of damping
α_D = damping constant that includes all sources of damping except that caused by the additive in question (Al or Al_2O_3)
δ = ρ_g/ρ
η = dynamic viscosity of combustion gas
γ = ratio of heat capacities of combustion gas c_p/c_v
ν = kinematic viscosity of combustion gas
ρ = density of particles suspended in combustion gas
ρ_g = density of combustion gas in chamber
ρ_s = density of propellant
ω = angular frequency of oscillations
u/ϵ = response function of combustion zone

Received by ARS August 24, 1962; revision received April 15, 1963. The authors wish to acknowledge the financial support of the Special Projects Office of the Bureau of Naval Weapons, the technical support of E. W. Price, and the contribution of Billy G. Brown, who carefully made all the firings.

* Chemical Engineer, Research Department.
† Physicist, Research Department.

Introduction

OSCILLATORY combustion, a problem that long has plagued the designers of rocket motors, owes its existence to the ability of the combustion process to couple with disturbances in the gas in such a way that a small perturbation can develop into high amplitude oscillations. These oscillations are usually in the normal acoustic modes of the rocket motor chamber. Oscillatory combustion, then, is the phenomenon in which the combustion chamber of a rocket motor exhibits the behavior of a self-excited oscillator. The balance of the paper will be devoted to the problem as it exists in solid propellant motors.

Over the years, various mechanical means have proved effective in increasing the acoustic losses in the rocket combustion chamber so that the oscillations are attenuated or eliminated. More recently, it has been found that various additives, such as aluminum, aluminum oxide, and silicon dioxide,[1] mixed into the propellant often will suppress the oscillations. By far the most important of these additives, because of its effectiveness and widespread use as a propellant fuel, is aluminum.